A 3-stage approach to derive key elastic properties for marine reservoir with faulted overburden

Yang Song, Yan Liu, Bing Bai, Lingli Hu, CGG*
Michelle Abraham, Yafei Wu, Anadarko Petroleum Corporation

Summary

Seismic inversion transforms seismic reflection data into quantitative rock-property descriptions of a reservoir, e.g., P-impedance, S-impedance, and density. Regardless of the inversion method used, the accuracy of and confidence in the inversion results rely highly on the quality of gathers or stacks obtained from seismic imaging.

Seismic data bandwidth is limited by signal-to-noise ratio (S/N), absorption, source wavelet, and shot and receiver ghosts. As a result, conventional seismic data lack low frequencies below 7 Hz. A typical deterministic seismic inversion workflow uses the low frequencies of existing well logs by extrapolating or interpolating along stratigraphic layers. The interpolation result is often biased on the well locations and quality of the well logs and can be affected by the interpolation method.

We propose a 3-stage method to minimize the dependency of seismic inversion on a well-log based initial model and improve confidence in the final result. The method includes 1) pre-migration deghosting to remove ghosts in the seismic data, subsequently extending seismic signal to lower frequencies; 2) high-resolution velocity model building with full waveform inversion (FWI) and fault-constrained tomography (FCT) to improve velocity resolution, extending the spectrum to higher frequencies; and 3) simultaneous seismic inversion using the FWI-derived model as the initial model to invert for P-impedance and Vp/Vs.

Introduction

Lithology, rock properties, and fluid identifications are critical for reservoir characterization, and retrieving this information is the ultimate goal of seismic data processing. A high-frequency full wave inversion (FWI) using a viscoelastic engine is ideal for this case, as it can truly mimic the scheme of how waves are propagated, transformed, attenuated, and recorded as seismic data. It therefore derives the most accurate viscoelastic properties of the earth. However, this process is very computationally expensive and currently not practical, especially for high frequencies. Lu et al. (2016) proposed a 2-stage FWI flow with an acoustic engine to derive high-frequency P-impedance. This is a simplified workflow from the full viscoelastic waveform inversion, but the computational cost is still high.

Moreover, P-impedance alone may not be sufficient to distinguish between reservoir and background. Figure 1 shows a better separation of reservoir sands using a Vp/Vs vs. P-impedance cross plot than using P-impedance alone. Simultaneous inversion provides useful information, e.g., P-impedance, S-impedance, and density, to differentiate gas sands from other non-gas layers (Castagna et al., 1993) and to lend support to reservoir planning and risk analysis.

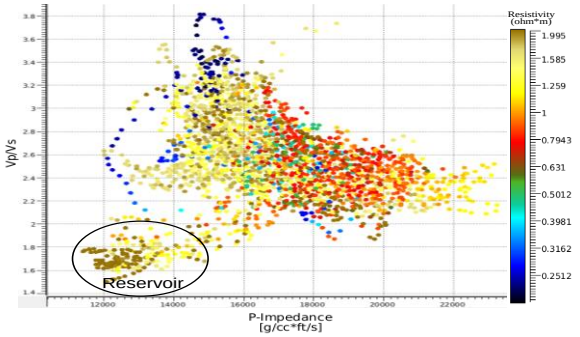

Figure 1: Vp/Vs vs. P-impedance cross plot colored by resistivity for a well in the study area from East Breaks, GOM. The plot is decimated to 2000 data points.

The computationally-effective flow for inverting P-impedance and Vp/Vs is through prestack simultaneous inversion using migrated common-image gathers (CIGs) and well logs. The inversion utilizes linearized Zoeppritz equations (Zoeppritz, 1919), such as the Fatti equation (Fatti et al., 1994), in 1D to be more cost-effective. A successful reservoir simultaneous inversion makes stringent demands on seismic data quality and assumes all 3D effects and amplitude distortion have been compensated prior.

Ideally, seismic data used for inversion should be noise-free, broad bandwidth, and with minimal amplitude distortion. However, none of these are true for real seismic data. Seismic data are usually contaminated by different types of noise. Seismic energy goes through various travel paths and forms multiples in addition to the primary reflection. The free-surface ghosts create notches in the frequency spectrum, thus limiting the seismic bandwidth. Effects such as spherical divergence, absorption, and transmission loss from geologic anomalies cause amplitude distortion. Various techniques have been developed to condition the migrated seismic data to be better suited for seismic inversion, such as structural filtering (Luo et al.,

2002; Singleton, 2009), stretching and offset-dependent tuning corrections (Lazaratos and Finn, 2004; Xu and Chopra, 2007), and inverse Q filtering (Zhang and Ulrych, 2007; Li et al., 2015).

Full bandwidth simultaneous inversion requires frequencies down to 0 Hz, which are not contained in typical seismic data. Combining a low-frequency initial model with the acquired seismic bandwidth is required to form a full bandwidth inversion result. The low-frequency initial model is usually built by extrapolating existing well logs along structural and stratigraphic horizons. The extrapolation is affected by the distribution of the well locations and the interpolation algorithms. It is only accurate around the well locations and is less reliable away from the wells.

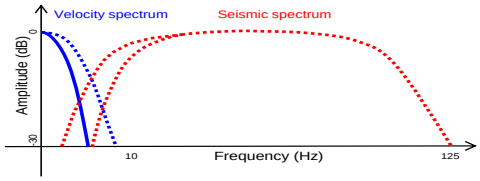

Figure 2: Schematic diagram of velocity and seismic spectra. The solid lines indicate a typical velocity spectrum after ray-based tomography and seismic spectrum under the impact of free-surface ghosts. The dotted lines indicate desired velocity spectrum after high-resolution velocity model building and seismic spectrum after ghost wavefield elimination.

In this study, we pursue another route to resolve the low frequency information that is missing from typical seismic data. A velocity model for seismic migration contains 3D subsurface information close to 0 Hz; however, its bandwidth is limited to very low frequencies when it is derived from ray-based tomography. As a result, there is a gap between the velocity and seismic data spectra (solid lines in Figure 2). In an effort to increase the bandwidth of both the seismic data and velocity model to fill in the spectrum gap (dashed lines in Figure 2), we propose a 3-stage seismic inversion flow: 1) broaden the seismic bandwidth using pre-migration deghosting; 2) increase velocity resolution using a high-resolution model building flow, which includes FWI and fault-constrained tomography (FCT); and 3) perform prestack simultaneous seismic inversion using the high-resolution velocity model as the initial model to invert for P-impedance and Vp/Vs. Initial Vs and density are calculated from initial Vp with empirical functions and loosely calibrated with a few wells. Thus, the derived impedance models do not strictly depend on the geologic structure defined by the interpreted horizons. In this paper, we use a narrow azimuth (NAZ) data set from East Breaks, Gulf of Mexico (GOM) to demonstrate the uplift of this seismic inversion workflow.

Marine reservoir with highly faulted overburden

The study area is located at East Breaks, GOM, about 150 miles south of Houston, TX. This field was first discovered in 1999 and has been producing both gas and oil since 2002. The reservoirs are located on a series of structural highs along a salt hinge line (Pan, 2002). The target sits between stair-stepping NNE-SSW trending normal faults on the western edge of a large mini-basin. The geologic challenge is the presence of many shallow gas clouds and faults (Figure 3). Due to the small size and irregular shape of the gas clouds and fault blocks, conventional ray-based tomography fails to capture the rapid velocity variation, and the underlying seismic image is distorted.

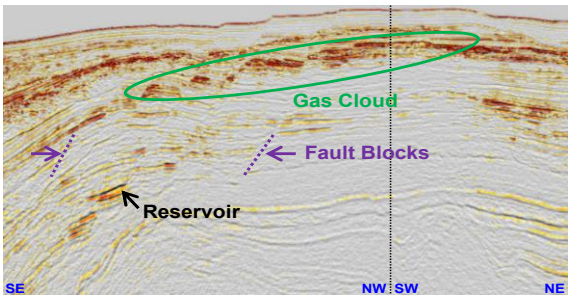

Figure 3: Presence of shallow gas clouds and abundant faults above and around the reservoir layer on perpendicular sections.

The data used for study is a 2007 NAZ survey with an 8400 m maximum offset. The source and receiver depths are 7 m and 9 m, respectively. A 1997 NAZ survey was used to infill acquisition holes. Frequency analysis shows that both low and high frequencies of the acquired data are limited by ghost notches (Figure 4, solid blue line). In the following sections, we will outline the three key stages for producing better reservoir inversion results.

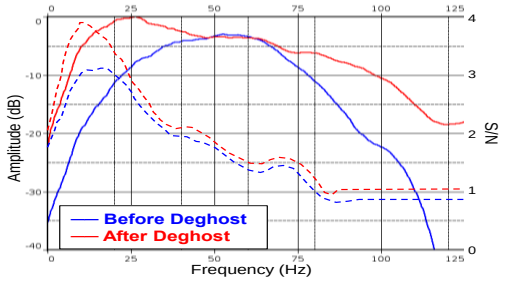

Figure 4: Amplitude spectra (solid lines) and S/N (dashed lines) comparison before (blue) and after (red) deghosting.

Pre-migration deghosting to broaden seismic bandwidth

To compensate for the frequency loss due to ghost notches, pre-migration deghosting using a bootstrap approach in the

Tau-P domain was applied to the input data (Wang et al., 2013). The amplitude spectra comparison in Figure 4 (shown by the solid lines) demonstrates that deghosting effectively broadened the bandwidth at both the low and high ends. The S/N (shown by the dashed lines) was also improved, particularly from 5 to 20 Hz. To better illustrate the effect of deghosting on low frequencies, a 0-2 Hz initial model was used for seismic impedance inversion. Figures 5a and 5b show the inverted P-impedance before and after deghosting compared with the well log at different frequency bands. The improved S/N after deghosting yields a better match between the extracted pseudo-log and the corresponding P-impedance well log. For low frequency bands, the reservoir events are more coherent and more consistent after deghosting (Figure 5d) than before deghosting (Figure 5c). Thus, we gained more usable low frequencies in the seismic data after deghosting.

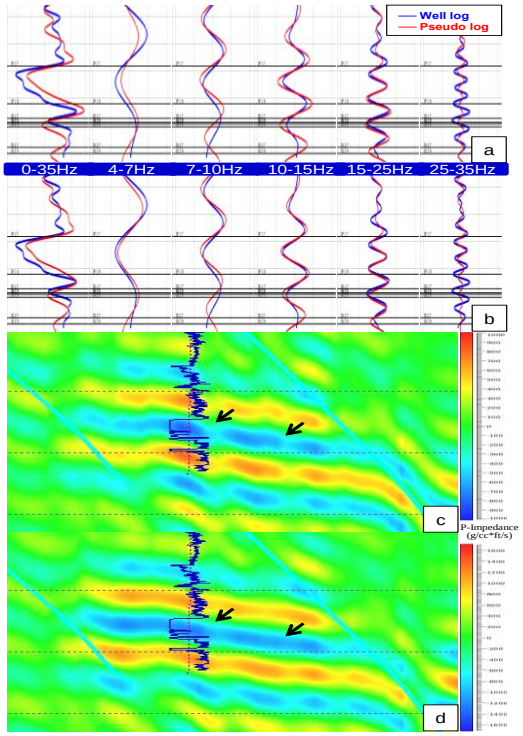

Figure 5: Band-pass filtered pseudo-log (red) extracted from P-impedance inversion compared with band-pass filtered well log (blue) before (a) and after (b) deghosting; 4-7 Hz band-pass filtered P-impedance inversion with well log overlaid before (c) and after (d) deghosting; the black arrows indicate a more continuous event after deghosting.

High-resolution velocity model building

Seismic inversion or AVO analysis requires flat CIGs. A proper migration velocity that generates flat CIGs is far superior to any post-migration gather flattening techniques which cannot correct amplitude and structure distortions caused by velocity errors. This is especially true for the complex overburden area in our study.

To build a high-resolution velocity model that honors the rapid velocity changes across gas clouds and faults, several velocity model building methods were applied. FWI with an acoustic engine was applied to resolve velocities for localized gas clouds and the faulted overburden. Given the limited cable length, the refraction FWI had a less reliable update for the depths below 3 km, so FCT was applied on top of FWI to refine the velocity model of the fault blocks. Within our testing area, over 100 fault horizons were interpreted, and FCT utilized these as constraints in ray-based tomographic velocity inversion to prevent velocity leakage across the faults.

Figure 6 shows the velocity and migration stack before and after FWI and FCT. Although our model without FWI is a legacy final model after several iterations of conventional ray-based tomography, it still lacks details. FWI and FCT successfully identified the location and shape of shallow gas clouds and produced a velocity model that honors the geology while preserving the sharp truncations against faults (Figure 6a and 6b). Particularly, FWI identified the slow velocity at the reservoir level. The faults and reservoir events are sharper and more continuous in the Kirchhoff migration images (Figure 6c and 6d). The higher resolution in the FWI model extends the velocity to higher frequencies to further close the gap between the velocity and seismic data spectra and provides more reliable low-frequency initial models for inversion.

Prestack simultaneous inversion

To better prepare for prestack simultaneous inversion, the input data were fully processed before migration, including various noise attenuations and surface-related multiple elimination (SRME) to remove coherent and random noise. Since shallow gas clouds were identified by FWI, Q tomography was implemented to invert for anomalous Q values associated with those gas clouds (Xin and Hung, 2009; Liu et al., 2014). A Q-PSDM Kirchhoff migration was used to compensate the corresponding phase shift and amplitude distortion to further improve the amplitude fidelity. Then we performed simultaneous seismic inversion on the migrated CIGs for P-impedance and Vp/Vs. Our 0-0-4-6 Hz initial models were based on the FWI/FCT velocity model, loosely calibrated with well logs around the reservoir level. Figure 7 shows the 0-2-30-40 Hz band-pass filtered P-impedance (Figure 7a) and Vp/Vs (Figure 7b) in a cross section passing through 6 wells. The inversion results conformed to the geologic structure and matched the well logs very well.

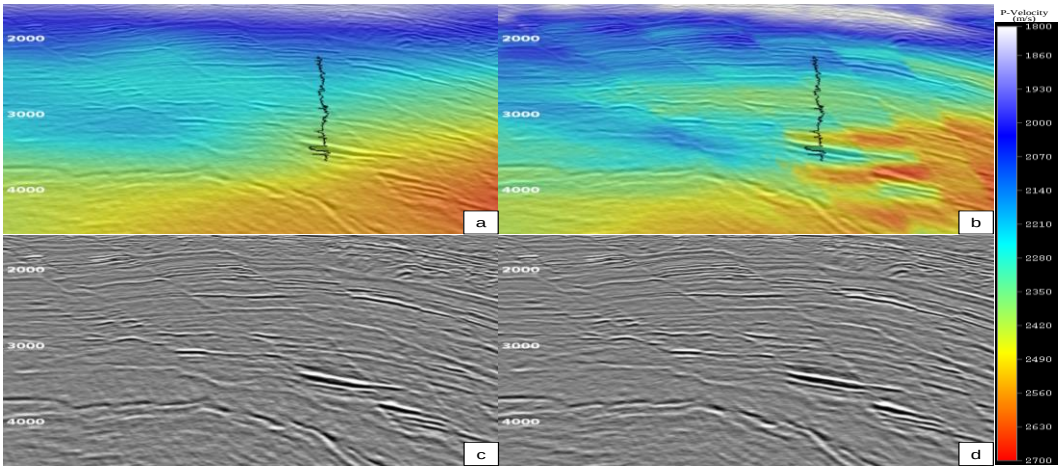

Figure 6: Velocity model before (a) and after (b) FWI and FCT, with P-wave sonic log overlaid as black curve (low velocity on left and high velocity on right); Kirchhoff migration stack before (c) and after (d) FWI and FCT.

Conclusions

We used a field data example from a reservoir with faulted overburden in East Breaks, GOM to demonstrate a 3-stage seismic inversion flow, which focused on filling in the spectrum gap between the low-frequency velocity model and the seismic data. Premigration deghosting was able to broaden the seismic data bandwidth and improve S/N, especially at low frequencies, thus improving the corresponding band-limited inversion result. The high-resolution velocity model, which was derived using FWI and FCT, honored the rapid velocity changes across shallow gas clouds and faults and resulted in less distorted structures. The velocity model had better lateral and vertical resolution and was used as the initial model for prestack inversion. With the combined benefits of deghosting and a high-resolution velocity model, the dependence of the seismic inversion on well log data and interpolation algorithms was reduced. The final prestack simultaneous inversion result matched well logs very well, and the interpretability of the seismic data was greatly improved.

Acknowledgments

We thank Anadarko and CGG for permission to present the results, and Seitel for providing input data for the infill area. We also thank Charles Contrino and Mark Chang for encouragement to carry out the study. We appreciate Rick Webster and David Barnett for their contribution in this study. We are grateful to Tony Huang, Qing Xu, Gabino Castillo, and Tsuyoshi Arikuma for their insightful discussions and suggestions.

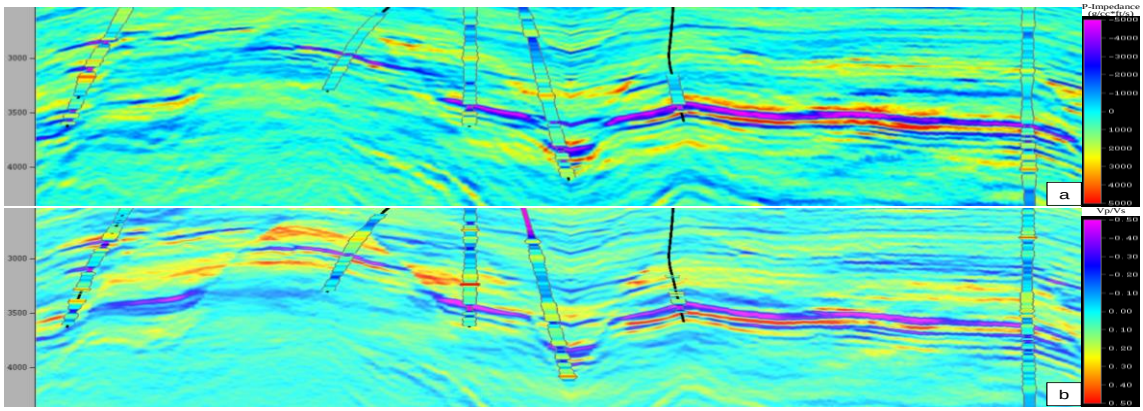

Figure 7: 0-2-30-40 Hz band-pass filtered P-impedance (a) and Vp/Vs (b) after simultaneous inversion on a polyline passing through 6 wells. The corresponding P-impedance and Vp/Vs well logs from the wells are overlaid on top.